CHIN. PHYS. LETT. Vol. 38, No. 4 (2021) 046301

Zintl Phase BaAgSb: Low Thermal Conductivity and High Performance Thermoelectric Material in *Ab Initio* Calculation

Shao-Fei Wang(王绍菲)[1,2,3], Zhi-Gang Zhang(张志刚)[4,5], Bao-Tian Wang(王保田)[1,2,6], Jun-Rong Zhang(张俊荣)[1,2,3*], and Fang-Wei Wang(王芳卫)[2,3,4,5*]

[1]*Institute of High Energy Physics, Chinese Academy of Sciences, Beijing 100049, China*
[2]*Spallation Neutron Source Science Center, Dongguan 523808, China*
[3]*School of Nuclear Sciences and Technology, University of Chinese Academy of Sciences, Beijing 100049, China*
[4]*Beijing National Laboratory for Condensed Matter Physics, Institute of Physics, Chinese Academy of Sciences, Beijing 100190, China*
[5]*Songshan Lake Material Laboratory, Dongguan 523808, China*
[6]*Collaborative Innovation Center of Extreme Optics, Shanxi University, Taiyuan 030006, China*

(Received 29 January 2021; accepted 2 March 2021; published online 6 April 2021)

Thermoelectric materials are critical parts in thermal electric devices. Here, Zintl phase BaAgSb in space group of $P6_3/mmc$ is reported as a promising thermoelectric material in density function theory. The anisotropic lattice thermal conductivity and phonon transport properties are investigated in theory. The strong phonon-phonon scattering in BaAgSb exhibits ultra-low lattice thermal conductivity of $0.59\,W\cdot m^{-1}\cdot K^{-1}$ along c-axis at 800 K, and high thermoelectric performance ZT = 0.94 at 400 K. The mix of covalent and ionic bond supports high carrier mobility and low thermal conductivity. The unusual features make BaAgSb a potential thermoelectric material.

DOI: 10.1088/0256-307X/38/4/046301

Zintl phase compounds have attracted tremendous interests for their excellent thermoelectric properties. The complex Zintl phase compounds[1] with ionic and covalent bonding possess low lattice thermal conductivity and ideal carrier mobility. The covalent bond region provides 'electron-crystal' properties, and the ionic bond area creates 'phonon-glass' properties.[1] The adjustment of electronic transport and control of phonon scattering is separated by different regions. The split of function regions makes the high thermoelectric efficiency achievable by manufacturing process.

Several Zintl phase thermoelectric compounds have been reported,[2] and numerous efforts have been made to elevate the thermoelectric performance including doping,[3,4] alloying and manufacturing,[5,6] and so forth.[7,8] Even though various materials have been proposed with thermoelectric performance, the requirements of commercialized thermoelectric devices are unsatisfied. Therefore, it is still necessary to search novel Zintl phase compounds with excellent thermoelectric performance. Recently, Zintl phase compounds in space group of $P6_3/mmc$ have been reported as thermoelectric materials, such as $Yb_{14}MnSb_{11}$[9] and SrAgSb.[10] The intrinsic ultra-low thermal conductivity of these thermoelectric materials is probably coming from the effective phonon scattering by heavy atoms or vacancies.[1] The low thermal conductivity of Eu_2ZnSb_2[11] with high Zn vacancies results in the high thermoelectric performance (ZT∼0.6). Materials with low thermal conductivity is candidates of promising high-performance materials. SrAgSb as a relatively high ZT material is investigated experimentally.[10] Inspired by the study of several Zintl phase materials, the intrinsic thermoelectric performance of BaAgSb with the same space group of $P6_3/mmc$ is studied systematically in this work.

The first-principles calculations are performed by density function theory in Vienna *ab initio* simulation package (VASP).[12] The energy convergency criterion is set to 10^{-7} eV for the electron self-consistency, and the convergency criterion for Hellmann–Feynman forces is taken to be 0.001 eV/Å. The cutoff energy is set as 650 eV, and monkhorst-pack $9\times9\times9$ k-mesh is used for the first Brillion zone. The HSE06 hybrid function[13] is used to estimate the electronic band structure. The phonon transport properties are calculated according to the 2nd and 3rd interaction force constants with Phononpy[14] and Sheng-BTE package.[15] The electronic transport properties are performed in Boltztrap program.[16]

Zintl phase BaAgSb with lattice constants a = 4.991 Å and c = 9.386 Å is shown in Fig. 1. The ab plane is in-plane direction, and c-axis is named as out-

Supported by the National Key R&D Program of China (Grant Nos. 2016YFA0401503 and 2017YFA0403700), the National Natural Science Foundation of China (Grant Nos. 11675255, U1932220, 11675195, and U1932220), the Key Research Program of Frontier Sciences, CAS (Grant No. 292016YQYKXJ00135), and the Program of State Key Laboratory (Grant No. 12074381).
*Corresponding authors. Email: jrzhang@ihep.ac.cn; fwwang@iphy.ac.cn
© 2021 Chinese Physical Society and IOP Publishing Ltd

plane direction. Ag forms nearly covalent bond with Sb, Ba is ionic bonding with AgSb clusters, and each Ba denotes 1.2 electrons to AgSb clusters. Ba, Ag, Sb occupy the 2*a*, 2*c*, and 2*d* sites, respectively. The Ba layer is located on the center of the AgSb layer with hexagonal close-packed (hcp). The bond length between Ba–Ag/Sb is 3.677 Å, which is longer than the Sb–Ag (2.843 Å) bond. The large layer distance (4.666 Å) of Ba and AgSb layers indicates the possible weak interaction. The BaAgSb provides larger crystal volume and heavier 2*a*-site atoms than SrAgSb. This produces loosely bond and gentle vibrations in BaAgSb. Materials with soft vibrations may have lower thermal conductivity, and the thermal electric performance of BaAgSb is evaluated in the following.

The electronic band structure with indirect band gap of 0.54 eV is shown in Fig. 2. The carrier effective mass m^*, which relates to the second-order partial derivative of band structure edge, is usually used to discuss the mobility of electrons in the periodic potential filed of crystal. According to electronic band structure, the carrier effective masses are calculated. The electron effective masses are 0.3 and 0.74 m_e, and hole effective masses are 0.19 and 0.47 m_e, along in-plane direction and out-plane directions, respectively. The different electron/hole effective masses along different directions indicate the anisotropic electronic transport property. The lower carrier effective masses suggest the domination of carrier transport along in-plane direction, as demonstrated in Figs. 3(b) and 3(e). In comparison with α-MgAgSb,[17,18] the electronic band edge of BaAgSb are more steeply. The steeply band edge indicates the smaller carrier effective masses of BaAgSb, thus provides higher conductivity. High carrier conductivity is in favor of the thermoelectric performance.

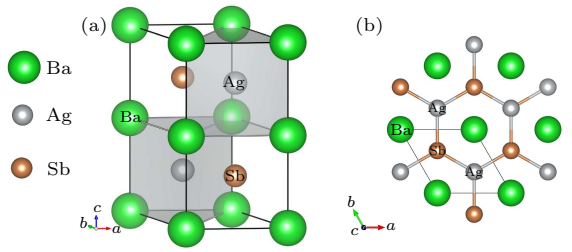

Fig. 1. The crystal structure of BaAgSb in side (a) and top (b) views. The green, silver and brown balls represent the Ba, Ag, Sb atoms, respectively.

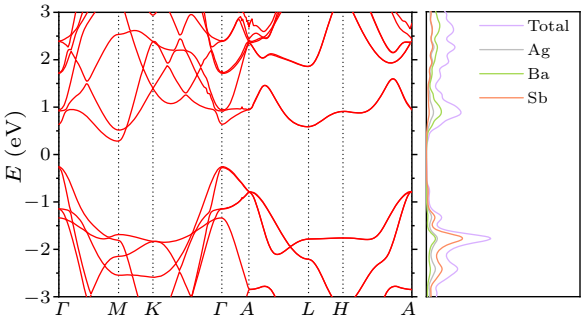

Fig. 2. The electronic band structure, the total and partial electronic density of states, which are calculated by HSE06 hybrid function. The gray, green and orange lines represent the contribution of Ag, Ba and Sb, respectively.

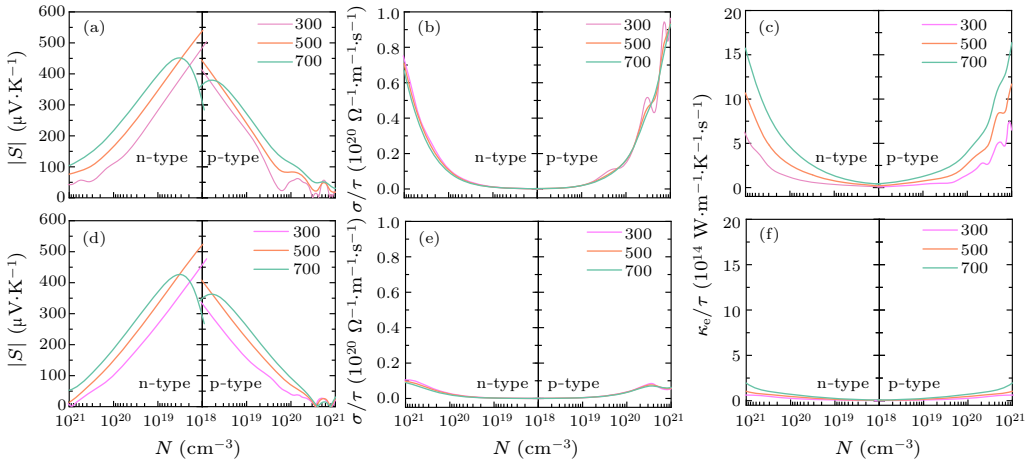

Fig. 3. Carrier concentration dependence of the electronic transport properties: seebeck coefficients S, electronic conductivity σ/τ, electronic thermal conductivity κ_e/τ, in the *ab* plane (a)–(c) and *c*-axis (d)–(f). The left and right parts in each figure correspond to the n-type and p-type doping.

The electronic transport properties are calculated according to the electronic density of states (DOS), as shown in Fig. 3. The evolution of seebeck coefficient S, electronic conductivity σ/τ, and electronic thermal conductivity κ_e/τ are displayed. With the elevation of carrier concentration, the Seebeck coefficient and electronic thermal conductivity are declined, while electronic conductivity is enhanced, because more carriers participate in the electrical conductivity. The Seebeck coefficient is larger along the in-plane direction, but electronic conductivity and electronic thermal conductivity are smaller in this direction. The different transport properties in two directions show the anisotropic property of BaAgSb.

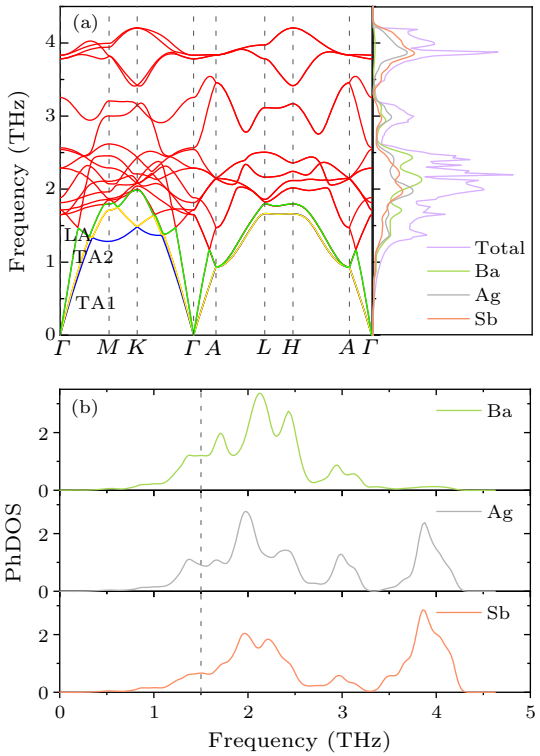

Fig. 4. The phonon dispersion curves (a) and partial phonon density of states (b).

According to $ZT = S^2\sigma T/\kappa$,[19] the thermoelectric conductivity κ makes visible effect on the thermoelectric performance, thus the phonon transport properties are analyzed. The phonon dispersion curves calculated by finite displacement method are shown in Fig. 4(a). Both high frequency optical and acoustic phonon indicate the stronger atomic vibrations in the L–H and M–K directions. The partial phonon density of states are selected to highlight the contribution of every element. Ag–Sb with covalent bond has smaller mass than Ba. High frequency vibration modes are produced by Ag–Sb cluster, which generate stronger vibrations under the same perturbation, as shown in Fig. 4(b). The low frequency vibration modes are mainly devoted by Ba and Ag, which is more obvious at around 1.3 THz. In comparison with other compounds, BaAgSb vibrates in the low frequency region, such as SnS_2 with the highest acoustic frequency nearly 3 THz, and the lowest optical frequency is around 10 THz.[20] This indicates the possibility of worse thermal transport ability. To our knowledge, materials with this kind of low frequent phonon dispersion curves are rare. Materials with flat phonon dispersion curves correspond to small phonon group velocities and difficult phonon transport processes. The cross of low frequency optical and acoustical branches produces large three phonon scattering phase space, thus provides high scattering possibility. A large amount of phonons exist in the crossing region, as shown in phonon density of states. This indicates the possible strong phonon scattering. The frequency of acoustic modes in BaAgSb are higher than those of α-MgAgSb,[21] thus deduces the possible higher thermoelectric conductivity.

Table 1. List of κ for other thermoelectric materials at 300 K.

Material	κ ($W{\cdot}m^{-1}{\cdot}K^{-1}$)	
BiTe	0.47	Ref. [22]
SnSe	0.9–1.0	Ref. [23]
$BiTe_{0.5}Se_{0.5}$	1.8–1.5	Ref. [22]
BiCuSeO	0.6–0.5	Ref. [24]
ZrS_3	2.82–15.63	Ref. [25]
α-MgAgSb	0.54	Ref. [17]
BaAgSb	1.56	This work

The phonon dispersion curves indicate the possibility of low lattice thermal conductivity κ of BaAgSb. The lattice thermal conductivity κ is calculated, as shown in Fig. 5. The electronic thermal conductivity is negligible at high temperature. The increase of inharmonic scattering with temperature leads to the decrease of lattice thermal conductivity. The discrepancy of κ along in-plane and out-plane directions indicates the anisotropic thermal transport properties and thermoelectric performance. The thermal transport is resisted along out-plane direction according to lower thermal conductivity κ. The room-temperature thermal conductivities κ are 2.67 and 1.56 $W{\cdot}m^{-1}{\cdot}K^{-1}$ in in-plane and out-plane directions, respectively. The κ is 0.59 $W{\cdot}m^{-1}{\cdot}K^{-1}$ when the temperature arrives at 800 K. This lower κ is beneficial to the thermoelectric conversion efficiency. BaAgSb possesses similar κ as high performance materials such as α-MgAgSb, as shown in Table 1.

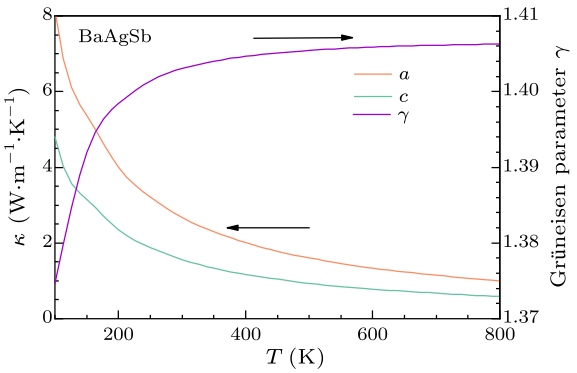

Fig. 5. The variation of lattice thermal conductivity κ and Grüneisen parameter γ with temperature. The orange line represents the in-plane κ, and the green line corresponds to the out-plane κ. The purple line shows the change of the γ according to temperature.

The calculated Grüneisen parameter γ shows the impact of temperature and reflects the intensity of inharmonic scattering, according to the purple line in Fig. 5. The room-temperature γ_{RT} (1.40) is close to the strong inharmonic scattering of α-MgAgSb (1.51),[18] which emphasizes the strong inharmonic

scattering in BaAgSb. The γ reaches maximum values at about 400 K, which manifests the strong inharmonic properties of BaAgSb in low temperature. We speculate that BaAgSb has high thermoelectric performance at around 400 K.

The thermoelectric performance[26,27] is estimated according to the electron and phonon transport properties. The temperature dependence of ZT under the carrier doping concentration of $5 \times 10^{19} \sim 1 \times 10^{20}\,\mathrm{cm}^{-3}$ is shown in Fig. 6. The out-plane ZT approaches to maximum value of 0.94 at 400 K with carrier concentration in $7.59 \times 10^{19}\,\mathrm{cm}^{-3}$. The in-plane ZT reaches the maximum value of 0.85 at 550 K, and the corresponding carrier concentration is $9.79 \times 10^{20}\,\mathrm{cm}^{-3}$. The lattice thermal conductivity is 0.2 and $0.15\,\mathrm{W{\cdot}m^{-1}{\cdot}K^{-1}}$ for the in-plane direction and out-plane direction, when ZT arrives at the maximum. The ZT of BaAgSb is close to that of high performance material α-MgAgSb (1.1),[18] thus BaAgSb is a promising thermoelectric material. The carrier concentration in maximum ZT is achievable in experiments. Under the different carrier doping, n-type BaAgSb shows advantage in out-plane direction and p-type BaAgSb exhibits relative higher performance along the in-plane direction. To further improve the thermoelectric performance, techniques such as doping, alloying and nanostructuring can be applied.

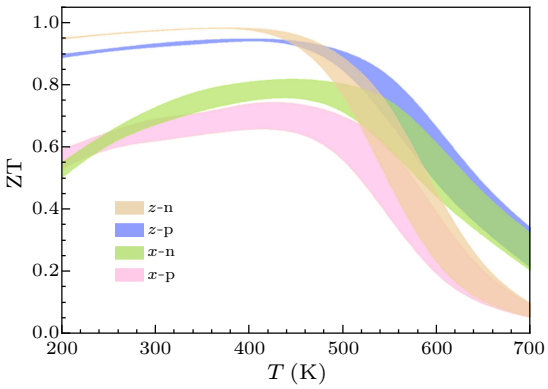

Fig. 6. The variation of ZT with respect to the temperature. The line width corresponds to the ZT in the carrier concentration from $5 \times 10^{19}\,\mathrm{cm}^{-3}$ to $1 \times 10^{20}\,\mathrm{cm}^{-3}$.

In conclusion, we have systematically investigated the thermoelectric performance of BaAgSb. The phonon dispersion properties and phonon-phonon scattering performance are evaluated. The low frequency phonon dispersion and the cross of acoustic/optical modes indicate the possibility of strong phonon-phonon scattering. The larger Grüneisen parameter γ also confirms the strong inharmonic scattering in BaAgSb. The anisotropic thermal electric features are confirmed by the different effective carrier masses and lattice thermal conductivities along in-plane and out-plane directions. Ultra-low thermal conductivity ($1.56\,\mathrm{W{\cdot}m^{-1}{\cdot}K^{-1}}$ at 300 K) and the higher thermoelectric ZT (0.94 at 400 K) are good performance of BaAgSb. Overall, Zintl phase BaAgSb with ultra-low thermal conductivity is a candidate material for thermoelectric devices.

References

[1] Kauzlarich S M, Brown S R and Snyder G J 2007 *Dalton Trans.* **2007** 2099
[2] Toberer E S, Zevalkink A, Crisosto N and Snyder G J 2010 *Adv. Funct. Mater.* **20** 4375
[3] Ortiz B R, Gorai P, Krishna L, Mow R, Lopez A, McKinney R, Stevanovic V and Toberer E S 2017 *J. Mater. Chem. A* **8** 4036
[4] Ortiz B R, Gorai P, Stevanovic V and Toberer E S 2017 *Chem. Mater.* **29** 4523
[5] Gayner C and Kar K K 2016 *Prog. Mater. Sci.* **83** 330
[6] Yang D D, Tong H, Zhou L J and Miao X S 2017 *Chin. Phys. Lett.* **34** 127301
[7] Feng B, Li G Q, Hu X M, Liu P H, Li R S, Zhang Y L, Li Y W, He Z and Fan X A 2020 *Chin. Phys. Lett.* **37** 037201
[8] Zhang X, Liu J, Li Y, Su W B, Li J C, Zhu Y H, Li M K, Wang C M and Wang C L 2015 *Chin. Phys. Lett.* **32** 037201
[9] Brown S R, Kauzlarich S M, Gascoin F and Snyder G J 2006 *Chem. Mater.* **18** 1873
[10] Zhang W M, Chen C, Yao H H, Xue W H, Li S, Bai F X, Huang Y F, Li X, Lin X, Cao F *et al.* 2020 *Chem. Mater.* **32** 6983
[11] Chen C, Xue W H, Li S, Zhang Z W, Li X F, Wang X Y, Liu Y J, Sui J H, Liu X J, Cao F *et al.* 2019 *Proc. Natl. Acad. Sci. USA* **116** 2831
[12] Kresse G and Furthmüller J 1996 *Phys. Rev. B* **54** 11169
[13] Jochen H, Gustavo E S and Matthias E 2003 *J. Chem. Phys.* **118** 8207
[14] Laurent C, Atsushi T, Isao T and Gilles H 2011 *Phys. Rev. B* **84** 094302
[15] Li W, Carrete J, Katcho N A and Mingo N 2014 *Comput. Phys. Commun.* **185** 1747
[16] Madsen Georg K H and Singh David J 2006 *Comput. Phys. Commun.* **175** 67
[17] Li X Y, Liu P F, Zhao E Y, Zhang Z G, Guidi T, Le M D, Avdeev M, Ikeda K, Otomo T, Kofu M *et al.* 2020 *Nat. Commun.* **11** 942
[18] Ying P J, Liu X H, Fu C G, Yue X Q, Xie H H, Zhao X B, Zhang W Q and Zhu T J 2015 *Chem. Mater.* **27** 909
[19] Lu B Y, Liu C C, Lu S, Xu J K, Jiang F X, Li Y Z and Zhang Z 2010 *Chin. Phys. Lett.* **27** 057201
[20] Zhan S P, Zheng L, Xiao Y and Zhao L D 2020 *Chem. Mater.* **32** 10348
[21] Tan X J, Wang L, Shao H Z, Yue S, Xu J T, Liu G Q, Jiang H C and Jiang J 2017 *Adv. Energy Mater.* **7** 1700076
[22] Samanta M, Pal K, Waghmare U V and Biswas K 2020 *Angew. Chem.* **132** 4852
[23] Chang C, Wu M H, He D H, Pei Y L, Wu C F, Wu X F, Yu H L, Zhu F Y, Wang K D, Chen Y, Huang L, Li J F, He J Q and Zhao L D 2018 *Science* **360** 778
[24] Zhao L D, He J P, Berardan D, Lin Y H, Li J F, Nan C W and Dragoe N 2014 *Energy & Environ. Sci.* **7** 2900
[25] Wang C, Zheng C B and Gao G Y 2020 *J. Phys. Chem. C* **124** 6536
[26] Wu Y Y, Zhu X L, Yang H Y, Wang Z G, Li Y H and Wang B T 2020 *Chin. Phys. B* **29** 087202
[27] Zhu X L, Liu P F, Zhang J R, Zhang P, Zhou W X, Xie G F and Wang B T 2019 *Nanoscale* **11** 19923